Stiffness and Buckling Behavior of Woven Columns

Jaimie Krankel¹, Guowei Wayne Tu², and Evgueni T. Filipov^{1,2,*}

ABSTRACT

Woven shell structures are beneficial for applications requiring lightweight material, durability, and design tunability such as in smart material devices, soft robotics, and aerospace. A fundamental component of these structures is the woven column. While the mechanical properties of a woven column can be determined, existing models are computationally expensive and do not explain the underlying mechanics behind trends. This work establishes purely analytical models for the buckling load and stiffness of woven columns, as well as a criteria for the buckling modes of these columns. The results of our models match closely to experimental data across various weave design parameters, and through our buckling mode criteria we determine local and global buckling trends across weave parameters. Our model advances our understanding of mechanics in woven structures and serves as a baseline for design.

Keywords: analytical model, woven structure, shell buckling, local buckling

1 Introduction

The long-standing craft of weaving has gained traction in modern engineering industry for its mechanical strength, tunable nature, and light weight. These intrinsic properties of weaving are advantageous for smart material devices, soft robotics, and aerospace application ^{1–3}. The plain weave (Fig. 1a), in which perpendicular weavers alternate over and under each other, is the most commonly implemented pattern. This simple weave pattern achieves the tightest interlocking of material, making for strong and durable structures ⁴. Previous work shows that plain woven 3D shell structures have greater resilience than their continuous counterparts ¹, as demonstrated in Fig. 1b.

Similar to the continuous cylindrical shell, the woven column is a fundamental unit of 3D woven shell structures. Cylindrical shell buckling has been widely studied, and there exist closed form solutions for their behaviors^{5–7}. Woven column buckling behaviors, however, are more complicated due to local interactions between weavers (Fig. 1c). Recent works implement finite element analysis techniques^{8–11} and semi-analytical modeling^{12–14} to determine mechanical properties such as buckling load and stiffness of woven materials. These models can require large computational power, and unlike an analytical model, they do not help us understand the underlying mechanics of woven column buckling behaviors.

We derive purely analytical models for the stiffness and buckling forces of woven columns. We then classify global and local buckling modes of woven cylinders, and determine a relationship between the buckling mode and weaver width. Our models and findings explain scaling laws due to changes in weaver thickness and width, providing elegant tools for choosing suitable weaver parameters.

¹Deployable and Reconfigurable Structures Laboratory, Department of Mechanical Engineering, University of Michigan, Ann Arbor, MI, USA

²Deployable and Reconfigurable Structures Laboratory, Department of Civil Engineering, University of Michigan, Ann Arbor, MI, USA

^{*}E-mail: filipov@umich.edu

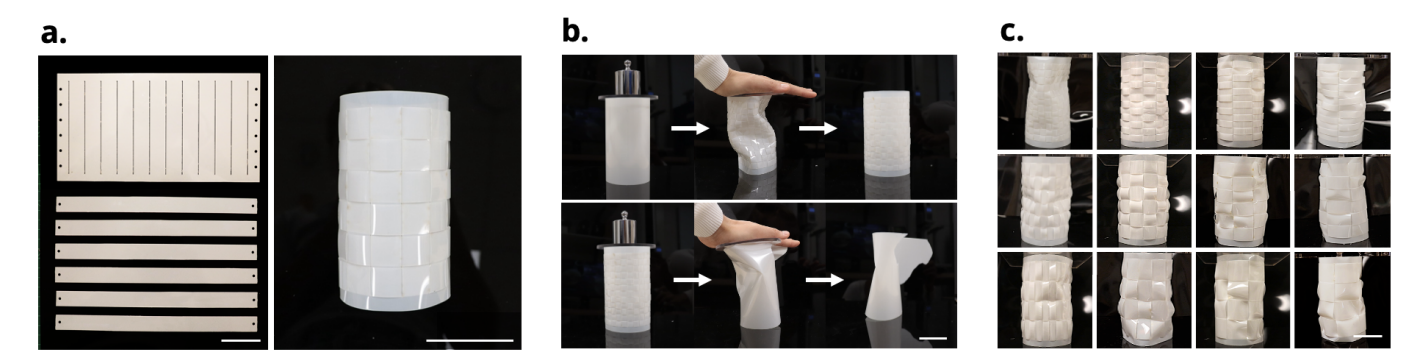


Figure 1. Overview of the woven columns and their buckling modes explored in this work. a. Construction of the plain woven column, a baseline architecture for 3D woven shell forms. **b.** Comparison shows that a continuous column undergoes permanent damage after buckling, whereas a woven column made of the same amount of material does not experience plastic deformation. **c.** Localized buckling of weavers contributes to overall buckling of columns. Buckling pattern is dependent on individual weaver parameters. Scale bars are 5 cm.

2 Mechanics model derivation

We use fundamental mechanics theory to derive models for the stiffness and critical buckling loads of a thin-walled, densely woven column. These models are based on geometric parameters and material properties of the column's vertical and horizontal weavers.

2.1 Buckling of woven columns

We assume that the critical buckling load of a woven column is the sum of the critical load of its vertical weavers and that of its horizontal weavers: $P_{cr, total} = P_{cr, h} + P_{cr, v}$. We first consider the critical load of vertical weavers $P_{cr, v}$. We assume that the weavers are initially straight and buckle independently. Furthermore, by assuming a densely woven cylinder, each segment of the vertical weaver is also independent. Illustrated in Fig. 2a, the buckling force of the combined vertical weavers is then governed by the buckling force of a singular segment. Based on the Euler buckling theory, $P_{cr, v}$ is dependent on the vertical weaver width w_v , vertical weaver thickness t_v , and horizontal weaver width w_h . 15

$$P_{cr, v} = n_v \frac{\pi^2 E \cdot w_v t_v^3}{w_h^2} \tag{1}$$

Next, we consider the critical load of the horizontal weavers $P_{cr, h}$. These weavers are assumed to be short cylindrical shells with axisymmetric sinusoidal deformations. Using classical theory, the critical load of a horizontal weaver is dependent on its thickness to radius ratio t_h/R and the face area A_f . Koiter's knockdown factor β accounts for deformations.⁶

$$P_{cr, h} = \beta \cdot \frac{E(t_h/R)}{\sqrt{3(1-v^2)}} \cdot A_f \tag{2}$$

Axisymmetric sinusoidal deformations greatly reduce the buckling force that a cylindrical shell withstands. To account for this, Koiter's knockdown factor β is solved implicitly using material parameters and the imperfection perturbation size δ_h^{16} .

$$\beta \cdot \left(\frac{\delta_h}{t_h}\right) = \left(\frac{4}{27}(1-v^2)\right)^{1/2}(1-\beta)^2 \tag{3}$$

The perturbation term δ_h can be calculated by approximating the horizontal weaver as a polygonal section with n_v sides of width w_v . Then δ is the average distance of this polygon from a circle of equal circumference.

Equivalently, we take half the distance of its maximum and minimum radii as in Fig. 2b.

$$\delta_h = \frac{1}{2} \left(\frac{w_v}{2\sin(\frac{\pi}{n_v})} + \frac{w_v}{2\tan(\frac{\pi}{n_v})} \right) \tag{4}$$

We compute the horizontal buckling force using Eqs. (2), (3), and (4). We can then add this to the buckling force of the vertical weavers Eq. (1) to obtain the total column buckling force.

2.2 Stiffness of woven columns

Considering the linear stiffness where the displacement is infinitesimally small, we assume that the stiffness of a woven column is the sum of the stiffness of its horizontal weavers k_h and the stiffness of its vertical weavers k_v : $k_{total} = k_h + k_v$. We will first consider the vertical weaver stiffness k_v . We assume that the vertical weavers deform sinusoidally as they are compressed, and that bending deformations store significantly more energy than axial deformations. These weavers act in parallel and resist bending deformations. The vertical weavers take on a curved cross section, which will increase their stiffness significantly by a factor α . We balance forces and moments at the location of the greatest perturbation (as in Fig. 2a) to obtain a dependence of the axial load of the weaver P_v on flexural rigidity EI, number of vertical weavers n_v , weaver curvature κ , and perturbation δ_v . Note that κ and δ_v are both functions of the axial displacement Δ . By relating stiffness to the derivative of axial load with respect to axial displacement, we obtain:

$$k_{\nu} = \alpha \cdot \frac{d}{d\Delta} \left[n_{\nu} EI \cdot \frac{\kappa(\Delta)}{\delta_{\nu}(\Delta)} \right] \tag{5}$$

The factor α accounts for the significant effect of curvature induced stiffness^{17–19}, which increases with vertical weaver width. We apply Pini's equation to the vertical weaver segments, using the column radius R.

$$\alpha = 10 + \frac{w_v^4}{60t_v^2} \left(\frac{v}{R}\right)^2 \tag{6}$$

Assuming the out-of-plane displacement δ_{ν} is small and that the vertical weaver deforms sinusoidally with n_h half waves, we determine the maximum curvature κ of the vertical weavers using the curvature formula. At maximum curvature, this reduces as follows:

$$\kappa = \delta_{\nu} \left(\frac{n_h \pi}{L - \Lambda} \right)^2 \tag{7}$$

Since $\kappa \propto \delta_{\nu}$, our derivative simplifies without further calculation of δ_{ν} and we simplify Eqs. (5), (6), and (7):

$$k_{\nu} = \left(10 + \frac{w_{\nu}^{4}}{60t_{\nu}^{2}} \left(\frac{\nu}{R}\right)^{2}\right) \cdot 2n_{\nu}EI\frac{(n_{h}\pi)^{2}}{(L-\Delta)^{3}}$$
(8)

Horizontal weavers act in series and deform axially in response to loading. The contact area A is the area where horizontal weavers make contact between vertical weavers, as shown in Fig. 2b. The horizontal weaver contribution to stiffness is then:

$$k_h = \frac{E n_v t_h^2}{n_h w_h} \tag{9}$$

We add Eqs. (8) and (9) to obtain the overall stiffness of a woven column.

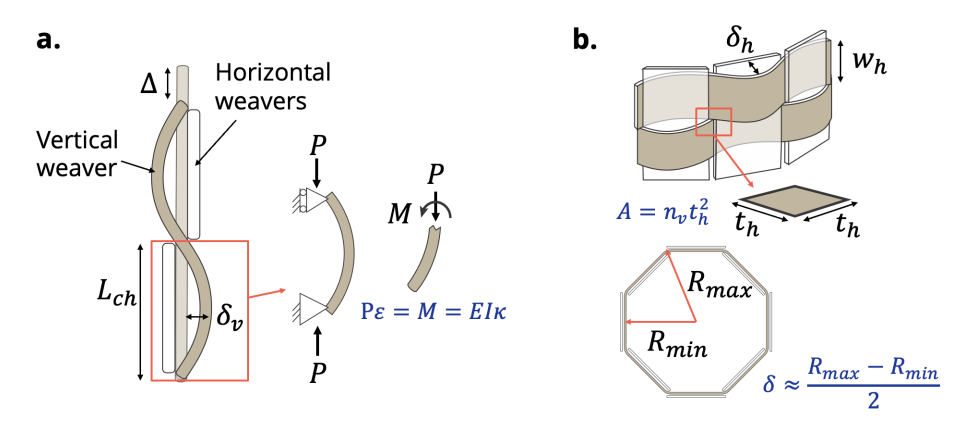
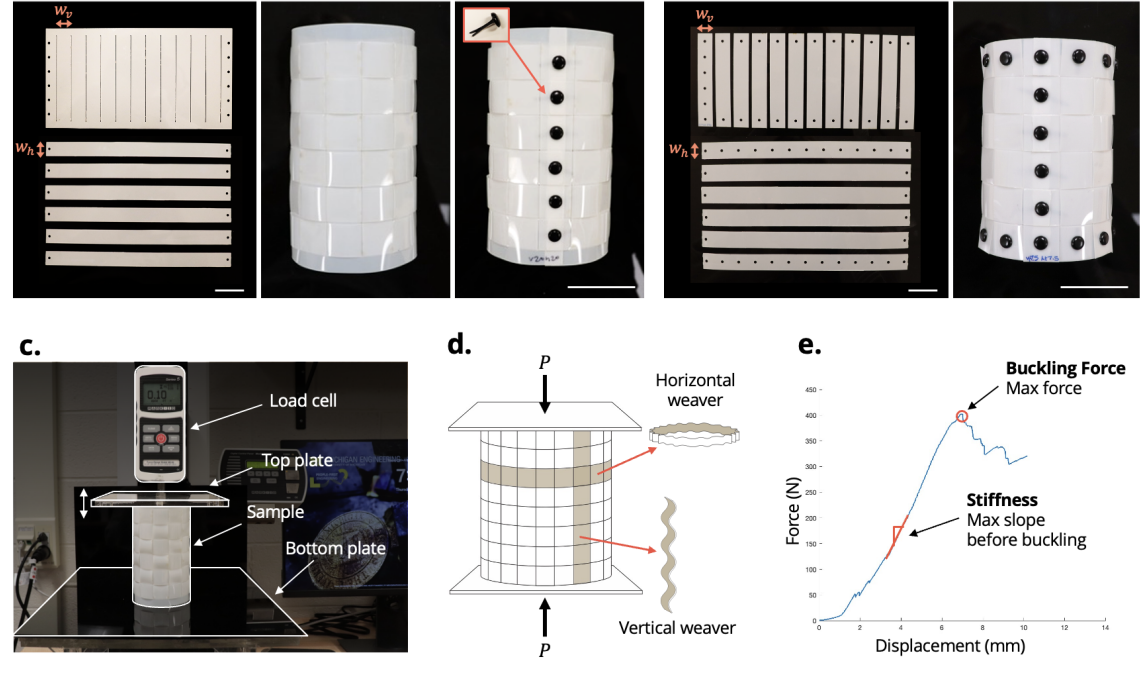


Figure 2. Derivation of the stiffness and buckling load of woven columns. a. Schematic of the vertical weaver. Each segment of the vertical weaver is modeled as an independent buckling beam. To derive stiffness, the inner force and bending moment are analyzed at locations of maximum curvature. **b.** Horizontal weaver schematic. Horizontal weavers are modelled as axisymmetric sinusoidally deformed cylindrical shells stacked on top of one another. Horizontal cross section is approximated as a polygon with n_{ν} sides for calculation of δ . Given a woven geometry, δ is derived by averaging R_{max} and R_{min} . Contact area for horizontal stiffness derivation is taken as the total contact area between subsequent horizontal weavers.

3 Sample fabrication and experimental methods

We conducted a parametric study and validated our models through physical experimentation on woven cylindrical shell samples. We constructed samples varying: (1) horizontal weaver width w_h , (2) vertical weaver width w_v , (3) horizontal weaver material thickness t_h , (4) vertical weaver material thickness t_v , and (5) sample height h. Our samples are woven by hand from vertical and horizontal strips of Mylar[®] polyester connected by a vertical seam of split pins (Fig. 3a). For studies with consistent vertical weaver thickness, the vertical weavers are cut from a continuous piece of material with a 10mm connection at the top and bottom This method assists fabrication and consistency in spacing, but may cause varying end effects if the vertical weaver thickness varies. In our study varying vertical thickness, we instead connect vertical weavers using two additional rows of split pins. We maintain consistent tightness of the weaving across all samples by scaling the distance between weavers proportionally to the weaver material thickness. 20,21

We obtained an experimental buckling force, stiffness, and qualitative buckling mode for each woven sample using plate-plate compression loading between two acrylic plates (Fig. 3b). The samples were compressed at a rate of 15 mm/min using a Mark-10[®] ESM 1500 single-column tabletop testing system with a 250 N load cell. Force and displacement are recorded at a sampling rate of 20 Hz until a global maximum force is reached. Buckling force is taken as the peak load experienced and stiffness is taken by numerically differentiating the data to find the maximum instantaneous slope before the buckling force is reached (See Fig. 3c). To account for precision error in sample fabrication, we tested three identical samples of each variation.



b.

Figure 3. Fabrication of woven columns and the test setup. a. For tests where vertical thickness remains constant, vertical weavers are connected at top and bottom to maintain consistent spacing in samples. Scale bars are 4 cm. **b.** For tests where vertical thickness varies, vertical weavers are joined directly at the top and bottom of horizontal weavers to maintain consistent end effects. Scale bars are 4 cm. **c.** Test setup using Mark-10[®] ESM 1500 single-column tabletop testing system. **d.** Schematic for plate-plate compression loading of woven column. Vertical and horizontal weavers both deform with sinusoidal deflections. **e.** Typical force-displacement curve. Measured properties are buckling force and stiffness.

4 Results

Parametric studies were performed by varying horizontal weaver width w_h , vertical weaver width w_v , horizontal weaver material thickness t_h , vertical weaver material thickness t_v , and sample height h. Qualitative trends in buckling behavior varied with respect to weaver widths, and larger vertical weaver widths correlated with local buckling modes and pre-buckling behavior. We validated our models for the buckling force and stiffness of woven columns against the experimental data.

4.1 Buckling mode classification

Based on our parametric study varying vertical and horizontal widths of woven columns, we observed correlations of global and local buckling in the samples (Fig. 4a) with vertical and horizontal weaver width. The locally buckling columns also commonly exhibited prebuckling behavior.

We define a column's buckling mode as global when the deformation immediately after buckling spans at least two horizontal weavers in width and at least two vertical weavers in height. If deformations are contained within individual weavers, we denote the column's buckling mode as local. We observed that columns of greater vertical width are more prone to local buckling behaviors, and columns of smaller vertical width are more prone to global buckling behaviors. Some columns of intermediate vertical weaver width exhibited both local and global buckling phenomena.

We define a column to be pre-buckle prone if it experiences any local maxima in its force-displacement curve before 95% of buckling force is reached. Local maxima are indicated when forces within 0.4 mm of a local maximum are less than 93% of this maximum. Columns that buckle in global patterns require for the

horizontal and vertical weavers to deform together causing failure of the system, whereas in local buckling patterns the locations of buckling are independent of one another and don't necessarily cause the overall failure of the column. Therefore, we observe more pre-buckling behavior in columns that buckle locally than in ones that buckle globally. This property may be more or less favorable depending on the application, but our results show that it can be tuned by adjusting the vertical weaver width.

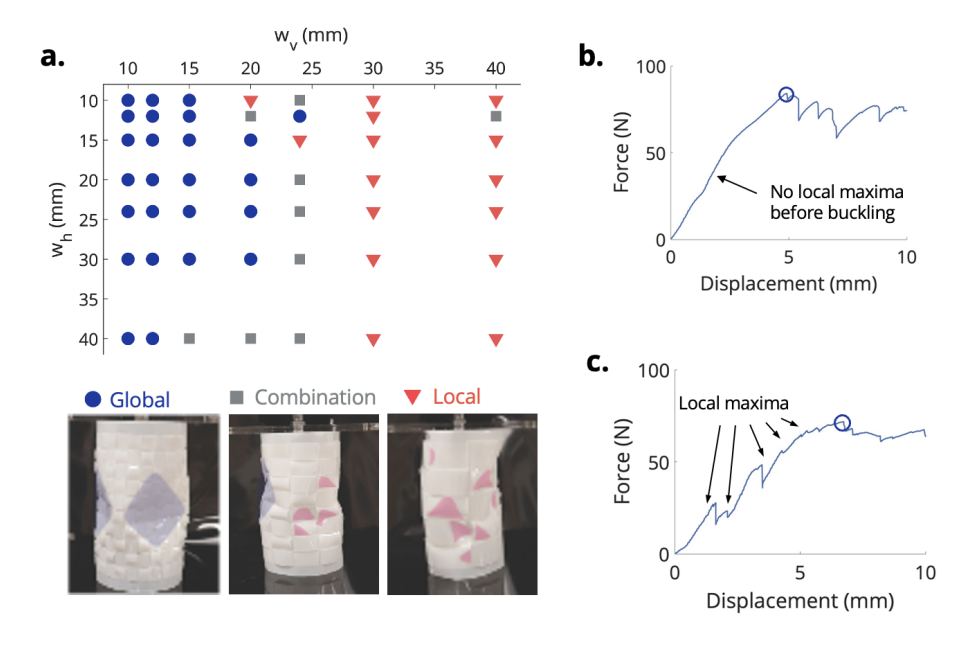


Figure 4. Comparison of buckling modes. **a.** Depending on a column's horizontal and vertical weaver widths, its buckling mode switches between global, local, and combination modes. **b.** Typical force-displacement curve for a globally buckling column. No pre-buckling behavior is experienced. **c.** Typical force-displacement curve for a locally buckling column. Pre-buckling is experienced before the maximum force is obtained.

4.2 Parametric study and model validation

The buckling force of a woven column increases with both its vertical and horizontal weaver thicknesses, as validated in Fig. 5a and b. By comparing Fig. 5a and Fig. 5b, we can determine whether the horizontal weaver thickness or vertical weaver thickness is more dominant based on which curve produces a greater buckling force. For thin structures (thicknesses less than 1.5 mm), the horizontal weaver thickness is more dominant than the vertical weaver thickness. For thicker structures (thickness greater than 3 mm), the vertical thickness is more dominant than the horizontal thickness.

Shown in Fig. 5d and e, our buckling force model is validated against variation in vertical and horizontal weaver width. Increases in vertical weaver width cause greater perturbations in horizontal weavers, making them more prone to buckling. When horizontal width is varied, our model assumes an ideal case in which the weaver spacing is consistent and weavers do not slip, hence no abnormalities can form on the column. If any vertical weaver has an irregular sinusoidal period, the largest wave will buckle first at a lower critical force than predicted. These defects become more likely when horizontal weavers are less wide, so a realistic fabricated column will not reach infinite buckling forces as the horizontal weaver widths become small. This effect on buckling force is most apparent in our data when horizontal and vertical widths are both less than 15 mm. Our model accurately predicts the near constant trend of the buckling force as horizontal width increases.

The effects of column height on buckling force are small compared to the effects of thickness factors. Similar to classical models for cylindrical shell buckling⁶, our model does not account for column height (see

Fig. 5c). Shown by the data, the columns of larger height buckle at lower forces than those of shorter height. As with shell buckling, this likely occurs due to the increased chance of fabrication defects and irregularities in longer columns.

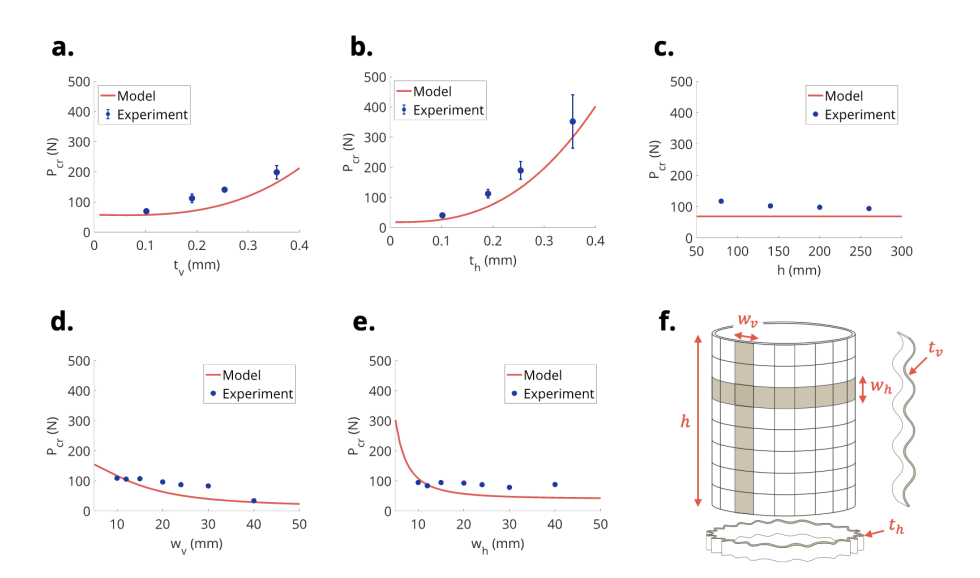


Figure 5. How different design parameters influence the buckling forces of woven columns. a. Buckling force increases proportionally to vertical thickness cubed, resulting from the relationship of vertical weaver buckling force to the second moment of inertia. **b.** Buckling force increases with horizontal thickness as a result of shell buckling. **c.** Buckling force experiences a slight decrease with height, which is not accounted for in the model. **d.** When vertical width increases, horizontal weavers experience greater deformation. This results in lower buckling forces for greater vertical weaver widths. **e.** Our idealized model expects that for small horizontal widths, the vertical weavers will experience tighter wave patterns resulting in higher buckling forces. In reality, inconsistencies in weaving allow for weak spots where the vertical weavers form larger waves. **f.** Schematic of design parameters.

The stiffness of the woven column increases with respect to both its vertical and horizontal weaver thicknesses, as validated in Fig. 6a and b. By increasing vertical weaver thickness, we increase the bending modulus of the vertical weaver by a factor of thickness cubed, hence making the structure stiffer. By increasing the horizontal weaver thickness, we increase the contact area between horizontal weavers, which also stiffens the structure. We compare Fig. 6a and b to determine whether the vertical weaver thickness or horizontal weaver thickness is more dominant in total structure stiffness. For thin structures (thicknesses less than 0.15 mm), the vertical weaver thickness is more dominant than the horizontal weaver thickness. For thicker structures (thicknesses greater than 0.25 mm), the horizontal thickness is more dominant than the vertical thickness.

Shown in Fig. 6d and e, our stiffness model is validated against variation in vertical and horizontal weaver width. As horizontal weaver width decreases, the vertical weavers are forced to have smaller periods with greater curvature relative to displacement, hence increasing stiffness of the vertical weavers and the overall stiffness of the column. As vertical weaver width increases, they curve more around the center of the column resulting in curvature-induced stiffness. In both cases, the vertical weavers contribution to stiffness causes the overall stiffness trend.

The increase in stiffness for shorter columns shown in Fig. 6c is related to the horizontal weaver contribution to stiffness. Our parametric study keeps horizontal weaver width constant, so we reduce height by stacking fewer horizontal weavers. Since the horizontal weavers act in series, a larger stiffness is achieved

when less weavers are stacked.

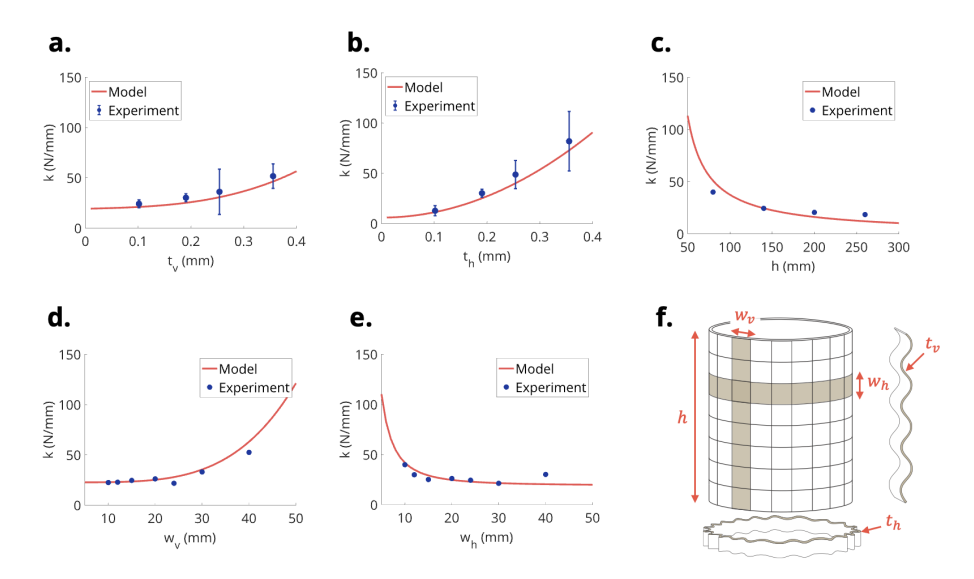


Figure 6. How different design parameters influence the stiffnesses of woven columns. a. Stiffness increases with vertical thickness, as a result of the relationship of k_{ν} to the vertical weaver second moment of inertia. b. Stiffness increases proportionally to horizontal thickness squared because the stress area $A_h \propto t^2$. c. Stiffness increases exponentially for shorter columns because by keeping w_h constant, we have $h \propto n_h$ hence the relationship follows from $k_h \propto \frac{1}{n_h}$. d. Stiffness increases with vertical weaver width because wider vertical weavers exhibit more curvature, resulting in additional curvature induced stiffness. e. As the horizontal weaver width decreases, the vertical weavers experience greater curvature relative to perturbation of shape. This results in increased stiffness. f. Schematic of design parameters.

5 Conclusions

We created purely analytic models for the buckling force and stiffness of woven columns, which are simple to use and have been parametrically validated against experimental data. Our models explain the underlying mechanics behind buckling force and stiffness trends in woven structures and serve as a closed-form tool for design. We determined that while both vertical and horizontal weavers contribute to the overall column buckling force and stiffness, in some cases one or the other will have more influence on tuning a property. Our results support effective design for efficient material use by identifying which weaving direction is dominant in achieving a desired structural property.

We established guidelines for the buckling mode of a column based on its vertical and horizontal weaver widths. We categorized columns into local and global modes, and determined that this trait is largely dependent on vertical weaver width. Based on the woven column's buckling mode, we determined its typical force-displacement relationship during compression testing. Our findings serve to guide design of woven structures such that favorable behaviors and buckling modes can be achieved.

References

- 1. Tu, G. W. & Filipov, E. T. Corner topology makes woven baskets into stiff, yet resilient metamaterials. *Phys. Rev. Res.* –, DOI: https://doi.org/10.1103/9srl-9gsc (2025). Accepted, in press, https://doi.org/10.48550/arXiv.2506.18197.
- **2.** Jing, K., Xie, S., Zhang, Y., Zhou, H. & Yan, H. Impact resistance of 3d woven fabrics and composites: A review. *Thin-Walled Struct.* **213**, 113262, DOI: https://doi.org/10.1016/j.tws.2025.113262 (2025).
- **3.** Wang, Z. & Sobey, A. Many-objective design optimisation of a plain weave fabric composite. *Compos. Struct.* **285**, 115246, DOI: https://doi.org/10.1016/j.compstruct.2022.115246 (2022).
- **4.** Abu Bakar, I. A., Kramer, O., Bordas, S. & Rabczuk, T. Optimization of elastic properties and weaving patterns of woven composites. *Compos. Struct.* **100**, 575–591, DOI: https://doi.org/10.1016/j.compstruct. 2012.12.043 (2013).
- **5.** Hilburger, M. W. Buckling of thin-walled circular cylinders. NASA Special Publication NASA SP-8007-2020/REV 2, NASA, Hampton, VA (2020). Revised version of NASA SP-8007 (1965).
- **6.** Gerasimidis, S., Virot, E., Hutchinson, J. W. & Rubinstein, S. M. On establishing buckling knockdowns for imperfection-sensitive shell structures. *J. Appl. Mech.* **85**, DOI: https://doi.org/10.1115/1.4040455 (2018).
- **7.** Ma, H., Jiao, P., Li, H., Cheng, Z. & Chen, Z. Buckling analyses of thin-walled cylindrical shells subjected to multi-region localized axial compression: Experimental and numerical study. *Thin-Walled Struct.* **183**, 110330, DOI: https://doi.org/10.1016/j.tws.2022.110330 (2023).
- **8.** Kumar, A. A., Hii, A. K., Hallett, S. R. & Said, B. E. Modelling woven composites with shell elements: An application of second-order computational homogenisation. *Comput. & Struct.* **312**, 107736, DOI: https://doi.org/10.1016/j.compstruc.2025.107736 (2025).
- **9.** Júnior, C. J. F., Nandurdikar, V., Neto, A. G. & Harish, A. B. Concurrent multiscale modelling of woven fabrics: Using beam finite elements with contact at mesoscale. *Finite Elem. Analysis Des.* **242**, 104274, DOI: https://doi.org/10.1016/j.finel.2024.104274 (2024).
- **10.** Nilakantan, G., Keefe, M., Bogetti, T. A., Adkinson, R. & Gillespie, J. W. On the finite element analysis of woven fabric impact using multiscale modeling techniques. *Int. J. Solids Struct.* **47**, 2300–2315, DOI: https://doi.org/10.1016/j.ijsolstr.2010.04.029 (2010).
- 11. Nguyen, Q. T., Nguyen, T. D., Dao, D. V., Le, D. V. & Nguyen, T. T. A study on mechanical properties of 3D printing abs plastic according to different printing orientations. *IOP Conf. Series: Mater. Sci. Eng.* 459, DOI: https://doi.org/10.1088/1757-899X/459/1/012082 (2018).
- **12.** Luo, D., Zhong, Y., Xi, S. & Shi, Z. Static, buckling, and free-vibration analysis of plain-woven composite plate with finite thickness using vam-based equivalent model. *Thin-Walled Struct.* **169**, 108503, DOI: https://doi.org/10.1016/j.tws.2021.108503 (2021).
- **13.** Dabiryan, H., Jesri, M., Ovesy, H. R. & Mazloomi, Z. S. Numerical and experimental study of buckling behavior of delaminated plate in glass woven fabric composite laminates. *J. Eng. Fibers Fabr.* **17**, DOI: https://doi.org/10.1177/15589250221091268 (2022).
- **14.** El Messiry, M. & El-Tarfawy, S. Mechanical properties and buckling analysis of woven fabric. *Textile Res. J.* **89**, 2900–2918, DOI: https://doi.org/10.1177/0040517518803777 (2018).
- 15. Hibbeler, R. Mechanics of Materials (Pearson, 2015).
- **16.** Koiter, W. The effect of axisymmetric imperfections on the buckling of cylindrical shells under axial compression. *Proc. K. Ned. Akad. Wet., B* **66**, 265–279 (1963).

- **17.** Pini, V. *et al.* How two-dimensional bending can extraordinarily stiffen thin sheets. *Sci. Reports* **6**, 29627, DOI: https://doi.org/10.1038/srep29627 (2016).
- **18.** Taffetani, M., Box, F., Neveu, A. & Vella, D. Limitations of curvature-induced rigidity: How a curved strip buckles under gravity. *Europhys. Lett.* **127**, 14001, DOI: https://doi.org/10.1209/0295-5075/127/14001 (2019).
- **19.** Barois, T., Tadrist, L., Quilliet, C. & Forterre, Y. How a curved elastic strip opens. *Phys. Rev. Lett.* **113**, 214301, DOI: https://doi.org/10.1103/PhysRevLett.113.214301 (2014).
- **20.** Banerjee, P. Principles of fabric formation (CRC Press, 2014).
- 21. Lord, P. Weaving: Conversion of yarn to fabric (Woodhead Publishing, 1982).